Characterisation of a new cell wall teichoic acid produced by *Listeria innocua* ŽM39 and analysis of its biosynthesis genes

Barbara Bellich, Nika Janež, Meta Sterniša, Anja Klančnik, Neil Ravenscroft, Roberto Rizzo, Jerica Sabotič, Paola Cescutti

PII: S0008-6215(21)00268-8

DOI: https://doi.org/10.1016/j.carres.2021.108499

Reference: CAR 108499

To appear in: *Carbohydrate Research*

Received Date: 18 October 2021

Revised Date: 26 December 2021

Accepted Date: 28 December 2021

Please cite this article as: B. Bellich, N. Janež, M. Sterniša, A. Klančnik, N. Ravenscroft, R. Rizzo, J. Sabotič, P. Cescutti, Characterisation of a new cell wall teichoic acid produced by *Listeria innocua* ŽM39 and analysis of its biosynthesis genes, *Carbohydrate Research* (2022), doi: https://doi.org/10.1016/j.carres.2021.108499.

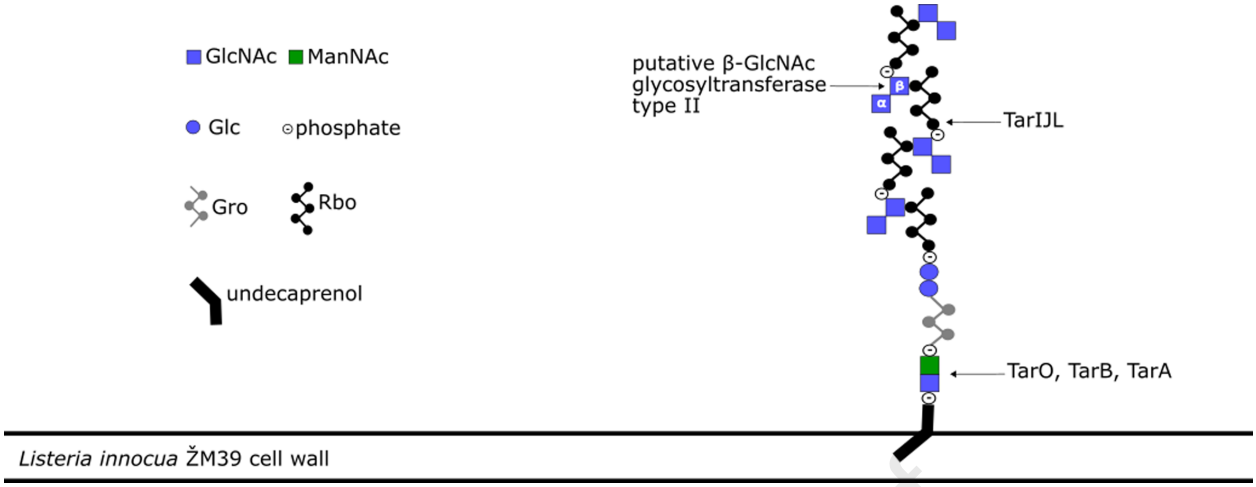

Characterisation of a new cell wall teichoic acid produced by *Listeria innocua* ŽM39 and analysis of its biosynthesis genes

Barbara Bellich [a,**], Nika Janež [b,**], Meta Sterniša [c], Anja Klančnik [c], Neil Ravenscroft [d], Roberto Rizzo [a], Jerica Sabotič [b,#], Paola Cescutti [a,*]

** B. Bellich and N. Janež equally contributed to this work

[a] *Department of Life Sciences, University of Trieste, via L. Giorgieri 1, Bdg. C11, 34127 Trieste, Italy*

[b] *Department of Biotechnology, Jožef Stefan Institute, Ljubljana, Slovenia*

[c] *Department of Food Science and Technology, Biotechnical Faculty, University of Ljubljana, Slovenia*

[d] *Department of Chemistry, University of Cape Town, Rondebosch 7701, South Africa*

* Corresponding author for the structural part
Paola Cescutti
Department of Life Sciences
University of Trieste
via L. Giorgieri 1, Bdg. C11
34127 Trieste, Italy
E.mail address: pcescutti@units.it
Tel: +39 040 5588755

[#] Corresponding author for the genetic part
Jerica Sabotič
Department of Biotechnology,
Jožef Stefan Institute, Jamova cesta 39
SI-1000 Ljubljana, Slovenia
E.mail address: jerica.sabotic@ijs.si
Tel: +386 1 477 3754

ABSTRACT

Listeria innocua is genetically closely related to the foodborne human pathogen *Listeria monocytogenes*. However, as most *L. innocua* strains are non-pathogenic, it has been proposed as a surrogate organism for determining the efficacy of antimicrobial strategies against *L. monocytogenes*. Teichoic acids are one of the three major cell wall components of *Listeria*, along with the peptidoglycan backbone and cell wall-associated proteins. The polymeric teichoic acids make up the majority of cell wall carbohydrates; the type of teichoic acids directly attached to the peptidoglycan are termed wall teichoic acids (WTAs). WTAs play vital physiological roles, are important virulence factors, antigenic determinants, and phage-binding ligands. The structures of the various WTAs of *L. monocytogenes* are well known, whereas those of *L. innocua* are not. In the present study, the WTA structure of *L. innocua* ŽM39 was determined mainly by 1D and 2D NMR spectroscopy and it was found to be the following:

$$[\rightarrow 4)\text{-}[\alpha\text{-D-Glc}p\text{NAc-}(1\rightarrow 3)]\text{-}\beta\text{-D-Glc}p\text{NAc-}(1\rightarrow 4)\text{-D-Rbo-}(1\text{P}\rightarrow]_n$$

This structure is new with respect to all currently known *Listeria* WTAs and it shares structural similarities with type II WTA serovar 6a. In addition, the genome of strain *L. innocua* ŽM39 was sequenced and the majority of putative WTA synthesis genes were identified.

Keywords: *Listeria innocua*; bacterial cell wall; wall teichoic acid; structure; NMR spectroscopy; teichoic acids synthesis genes.

1. Introduction

The genus *Listeria* consists of six *sensu stricto* and eleven *sensu lato* species. Two species, *Listeria monocytogenes* and *Listeria ivanovii*, pose a major risk to human health because infection with *L. monocytogenes* is associated with high rates of hospitalization and mortality compared to other foodborne infectious diseases [1]. *L. innocua* is genetically closely related to *L. monocytogenes*, but most strains are non-pathogenic, even though they are isolated from similar sources, tolerate extreme environmental conditions, and form biofilms. Therefore, *L. innocua* has been proposed as a surrogate organism for the study of the foodborne opportunistic pathogen *L. monocytogenes*, particularly to determine the efficacy of antimicrobial strategies against it [2-7]. *L. innocua* is considered a non-haemolytic saprophyte, that is widely distributed in the natural environment. Preventing the occurrence of *Listeria spp.* can be difficult because they are able to survive and adapt to stressors in different environments, such as food, soil, water, sewage, and mammalian hosts. They survive and persist in processing facilities and cause food contamination [8].

L. monocytogenes and *L. innocua* were traditionally identified by serotyping to distinguish between strains, and although this method is no longer used, serotyping data are consistent with differences in cell wall teichoic acid structures [9]. At least fourteen serovars are known for *L. monocytogenes*, while *L. innocua* strains have traditionally been typed as serovar 6.

The three major components of *Listeria* cell wall are teichoic acid polymers, the peptidoglycan backbone and wall-anchored and wall-associated proteins. Polymeric teichoic acids make up the majority of cell wall carbohydrates and are either directly bound to peptidoglycan and termed wall teichoic acids (WTAs) or tethered to the cytoplasmic membrane and termed lipoteichoic acids (LTAs) [9]. Teichoic acids play several important physiological roles in *Listeria*, including biofilm formation, control of cell division machinery, cation homeostasis, and function as phosphate reservoirs. They are also important virulence factors and antigenic determinants, as well as phage-binding ligands and therefore, they mediate interactions between bacteria, and with bacteriophages and eukaryotic host cells [9, 10]. The WTAs of *Listeria* are classified into two different types based on their structure. In type I WTAs, ribitol (Rbo) units are directly linked by phosphodiester bonds between C1 and C5, and may be decorated with terminal rhamnose (Rha) or N-acetyl glucosamine (GlcNAc) residues. Type II WTAs contain GlcNAc within the Rbo polymer chain, and this integrated GlcNAc may be decorated with glucose, galactose, another GlcNAc, or O-acetyl groups [9, 11-13]. The different structures of WTA, recently summarized by Sumrall et al. [9], are listed in Table 1 [14-18].

Currently, limited data on genetic diversity and WTA structures are available for *L. innocua*. The present work reports the primary structure of the WTA produced by the food isolate *L. innocua* strain ŽM39, which was mainly determined by 1D and 2D NMR spectroscopy of the native WTA. In addition, following genome sequencing, the majority of putative WTA synthesis genes were identified.

2. Results and Discussion

2.1. Purification and composition analysis of cell wall teichoic acids

Extraction of WTA from 30 mg of cell wall sacculi gave 7.8 mg of polymer. The sample was subjected to size exclusion chromatography and it eluted as a single peak; in order to reduce heterogeneity of the sample, only the central fractions of the peak were pooled together and used for structural analysis. Based on the calibration curve obtained with pullulan standards (Fig. S1), the WTA sample was estimated to have a MM of about 9700. This is a rough estimate as the anionic *Listeria* WTA has a very different structure and expected hydrodynamic volume and thus elution behaviour compared to neutral pullulan standards.

Composition analysis was determined by GLC of trimethylsilyl methyl glycoside derivatives; the gas chromatogram obtained only revealed the presence of GlcNAc.

2.2. NMR spectroscopy of cell wall teichoic acids

The ^{1}H NMR spectrum of *L. innocua* WTA is reported in Fig. 1. Two anomeric signals at 5.14 and 4.65 ppm were detected and assigned to residues **A** and **B**, respectively. The $^{1}J_{H1\text{-}H2}$ value of signal **A** is 3.4 Hz indicating that this residue has an α-anomeric configuration, while the $^{1}J_{H1\text{-}H2}$ value of signal **B** is 8 Hz, in agreement with a β-anomeric configuration. Integration of the peak area of **B** relative to **A** was 1.2, suggesting an equimolar ratio for the two components. The signal at 2.08 ppm was assigned to the methyl proton of N-acetyl groups in agreement with composition analysis; its integration value was 6 with respect to the anomeric proton of residue **A**, indicating that both residues are fully N-acetylated.

The repeating unit (RU) spin systems were determined using a combination of 1D and 2D ^{1}H-^{1}H correlation experiments. The anomeric region of the COSY spectrum gave H1 to H2 for residues **A** and **B** (Fig. S2), and also showed further correlations for two protons of the ring region: the resonance at 4.24 ppm correlated with two cross peaks at 3.84 and 3.62 ppm, while the resonance at

4.10 ppm showed correlations with signals at 3.99 and 3.82 ppm. 1D TOCSY experiments led to the assignments of most of the protons for the spin systems **A** and **B**. In fact, selective excitation of H1 of **B** (4.65 ppm) resulted in detection of H2 to H5 (Fig. 2), while selective excitation of the well isolated ring resonance at 3.54 ppm, assigned to H4 of the GlcNAc according to literature data, showed correlations to four other protons, H5 and H1 to H3, and revealed that it belongs to spin system **A**. As described later, the deshielded proton at 4.24 ppm assigned to H4 of **B** exhibited complex splitting due to coupling to the phosphodiester linkage. The assigned ^{1}H chemical shifts for spin systems **A** and **B** are reported in Table 2.

^{1}H–^{13}C correlation experiments (HSQC) (Fig. 3) led to the determination of all carbon atoms for the **A** and **B** spin systems. These assignments were confirmed by the HSQC-TOCSY correlations as shown in the expansion in Fig. S3: H1 of **A** and **B** to the corresponding C2 to C5 of each residue and H4 of B at 4.24 ppm to C1 to C6 of **B**. Inspection of the HSQC plot ring region (Fig. 3) showed some yet unassigned resonances, likely belonging to Rbo residue (**R**). In particular, the negative phased cross peaks at 4.10 - 3.99 ppm (^{1}H) and 67.3 ppm (^{13}C) were assigned to H1 of Rbo, while the cross peaks at 3.78 and /61.5 ppm (^{1}H/^{13}C) was attributed to H5/C5 of the same residue. The cross peak at 3.82/70.9 ppm (^{1}H/^{13}C) was assigned to H2/C2 of Rbo, since it correlated with Rbo H1 in the COSY spectrum (Fig. S2). The cross peaks at 3.82/71.7 and 3.91/82.7 ppm (^{1}H/^{13}C) are assigned to C3 and C4 of Rbo, with C4 strongly deshielded with respect to the non-substituted residue [19], indicating that it is a linkage position. 1D TOCSY experiments acquired with different mixing time values (80, 100, and 150 ms) with selective excitation of H1 of **R** at 4.10 ppm (in Fig. 2 the spectrum recorded with 100 ms mixing time is reported) further confirmed the assignments of Rbo ^{1}H and ^{13}C chemical shifts [20, 21], while in the HSQC-TOCSY plot C4 of **R** correlated with H3, H5, and H'5 of **R**, the latter at 3.86/61.5 ppm, thus completing the assignment for Rbo (Table 2).

The ^{1}H -^{13}C HMBC plot (Fig. S4) gave intra- and inter-residue correlations which confirmed the ^{1}H and ^{13}C assignments presented in Table 2 and established the linkages of **A** and **B** as follows. H1 of signal **A** correlated to C3 and C5 as expected for α-sugars and to the cross peak at 80.9 ppm assigned to C3 of **B**, whereas H1 of **B** correlates to the cross peak at 82.7 ppm assigned to C4 of **R**.

The ^{31}P spectrum showed one main resonance together with two small signals (Fig. S5) suggesting that, despite the purification process used, some heterogeneity of the sample was still present. The ^{1}H–^{31}P HMBC experiment (Fig. 4) revealed that the main ^{31}P signal correlated with a proton at 4.24 ppm, previously assigned to H4 of residue **B**, and with protons at 4.10 and 3.99 ppm which were attributed to H1 of **R** in the ^{1}H–^{13}C HSQC spectrum. These findings determined that the phosphodiester linkage is between C4 of β-GlcNAc and H1 of Rbo. Moreover, the cross peaks at

3.97 - 3.91 ppm (^{1}H) are correlated to a small ^{31}P resonance, but, unlike the main phosphodiester peak there are no additional correlations to residue B. Therefore, they were assigned to H1 of Rbo phosphomonoester, likely generated during the extraction process. Their ^{13}C chemical shift at 67.1 ppm in the ^{1}H–^{13}C HSQC spectrum (not labelled cross peaks in Fig. 3) is in agreement with such an assignment. The results obtained determined the RU structure of *L. innocua* WTA to be the following:

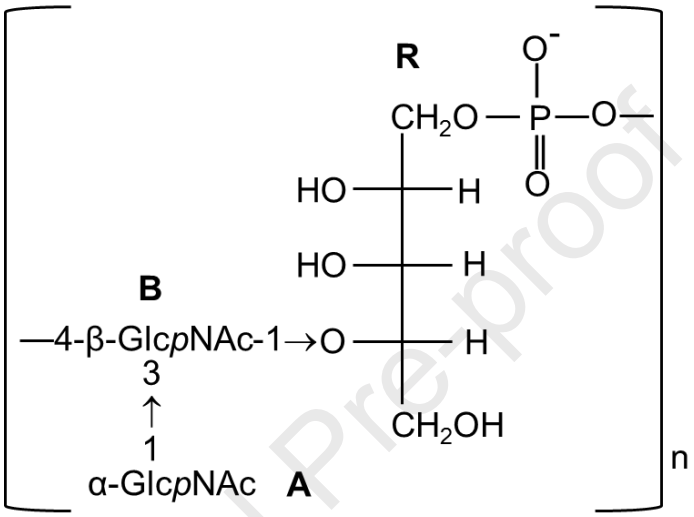

Scheme 1: Structure of the *L. innocua* ŽM39 WTA repeating unit

2.3. Identification of WTA biosynthesis genes in Listeria innocua ŽM39

The genome of *Listeria innocua* ŽM39 is 2.8 Mb long and has an average GC content of 37.4 %, similar to the reference strain *L. innocua* Clip 12662 [22] (Fig. S6). Plasmid-related sequences were not detected, but two complete (lmoS_188 and lmo_293) and one incomplete (A118) prophage sequences were identified in the genome (Fig. S6). There were 2843 protein-coding genes annotated, most of which (99 %) were genus-specific.

The WTA synthesis genes were predicted based on protein sequence homology to the WTA synthesis proteins of the prototype strain *Bacillus subtilis* 168 for the linkage unit, and of *Bacillus subtilis* W23 and *Staphylococcus aureus* 8325 for the polyribitol backbone [23]. Enzymes with glycosyltransferase activity (GT) involved in WTA biosynthesis were annotated based on homology to GTs of *S. aureus* and *L. monocytogenes* [17, 24-27].

In *Listeria*, WTA biosynthesis begins on the cytoplasmic side of the membrane, where the linkage unit GlcNAc-ManNAc-Gro is proposed to be synthesized by proteins homologous to

193 *Bacillus subtilis* TarO, TarA, and TarB, which are conserved among most Gram-positive bacteria,
194 including *Listeria* [23]. These proteins also have homologs in the genome of *L. innocua* ŽM39
195 (Table S1). Moreover, in *L. monocytogenes* TarO activity is carried out by two redundant TagO
196 genes (TagO1 and TagO2) [28] whose homologs have also been identified in *L. innocua* ŽM39 and
197 match homologs of *B. subtilis* TagO (Fig. 5, Table S1). For the synthesis of the polyribitol
198 phosphate backbone (Table S1) homologs of the proteins TarF, TarI, TarJ and TarL of *Bacillus*
199 *subtilis* W23 and *Staphylococcus aureus* 8325 were identified in *L. innocua* ŽM39: TarI and TarJ
200 synthesise CDP-ribitol, and TarL functions as a primase and polymerase that builds the polyribitol
201 chain, as reported for *S. aureus* [23] (Fig. 5).

202 Type II WTA are characterised by a β-GlcNAc linked to either C2 or C4 of Rbo [11, 30] and
203 in *L. innocua* WTA β-GlcNAc is bound to C4 of Rbo. The protein K1T44_1291 of *L. innocua* was
204 found to have a high homology (70.9 % identity, 99 % coverage) with the GT family 2 Liv1073
205 synthesized by *L. ivanovii* WCSL3009 and identified as a putative GT involved in the backbone
206 GlcNAc transfer. Moreover, the protein K1T44_1291 from *L. innocua* ŽM39 was found to be
207 homologous also to TarS, the GT involved in binding β-GlcNAc to C4 of Rbo in *S. aureus* strains
208 (Table S1) [23].

209 The GT involved in binding α-GlcNAc to C3 of β-GlcNAc, must act with a retaining
210 mechanism. Only two GTs of this type, have been identified in the genome of *L. innocua* ŽM39 and
211 they are homologs of LafA and LafB. However, based on homology data, these GTs are involved in
212 the LTA biosynthetic pathway (Table S2) and thus are unlikely to be involved in two different
213 processes occurring at different locations in the cell. An α-GlcNAc bound to the β-GlcNAc in the
214 backbone has been reported only in *L. innocua* serovar 6a WTA, but the GT involved in its addition
215 has not been described yet [11]. Currently, only the pathway for linking α-GlcNAc to Rbo in *L.*
216 *monocytogenes* serotype 1/2a has been elucidated. This process sequentially requires the
217 bactoprenol glycosyltransferase Lmo2550 which transfers GlcNAc to the lipid carrier, the flippase
218 GtcA, which flips the activated GlcNAc across the cytoplasmic membrane, and the action of
219 Lmo1079 which transfers α-GlcNAc to the growing WTA [27]. However, in *L. innocua* ŽM39 only
220 homologs of Lmo2550 and GtcA were identified, whereas that of Lmo1079 is absent (Table S1),
221 leaving this biosynthetic step unclear.

222 In *L. innocua* ŽM39 we identified a putative protein of the PMT family (K1T44_1285)
223 homologous to *L. monocytogenes* galactosyltransferase PmpA, which transfers Gal to the β-
224 GlcNAc (identity 68,6 %) in non4b serotype (WTA type II) [17]. Galactosylation of the non4b
225 serotype is also a multistep process similar to the addition of α-GlcNAc described above and is
226 carried out by the GalU, GtcB and GtcC proteins [17]. Their homologs were also identified in *L.*

innocua ŽM39 and their ORFs are complete, indicating that they are probably expressed as functional proteins, although no Gal decoration was detected in *L. innocua* WTA. Consistent with the WTA structure of *L. innocua* ŽM39, no proteins homologous to enzymes involved in glucosylation [31] and rhamnosylation [26] of *L. monocytogenes* WTA were identified (Table S1). The described WTA synthesis homologs were also identified in the model strain *L. innocua* Clip 11262 without major differences (Table S1), in agreement with the similarity between these two WTA structures. In fact, based on reaction with serotyping antibodies, *L. innocua* Clip 11262 was assigned to serotype 6a which is composed of the polyribitol phosphate chain substituted on C4 by β-GlcNAc which is further decorated by GlcNAc and galactose [11]. These data indicate that genetic characterisation alone may not reflect the actual glycotype, but rather implies glycosylation capacity, suggesting that direct determination of WTA structure is the only reliable method for characterization.

3. Conclusion

The WTA structure of *L. innocua* ŽM39 was determined by 1D and 2D NMR spectroscopy and consists of [→4)-β-GlcNAc*p*-(1→4)-Rbo-(1P) backbone with an α-GlcNAc*p* bound to C3 of the β-GlcNAc*p*. According to the current classification of *L. monocytogenes* WTA, the structure described for *L. innocua* ŽM39 WTA can be assigned to type II, since the β-GlcNAc residue is part of the backbone [11]. Decoration of β-GlcNAc by an α-GlcNAc occurs in stoichiometric amount, while no acetyl groups could be detected. This structure is similar to type II WTA serovar 6a which however contains a β-GlcNAc substituted in non-stoichiometric amounts with Gal, α-GlcNAc and acetyl groups. Furthermore, serovar 6a was determined by mass spectrometry [11] (Table 1), while our work reports the complete NMR assignment of WTA repeating unit. *L. innocua* ŽM39 produces a new type of structure of WTA, but only an immunological approach can establish if it should be recognized as a new serotype.

In addition, we identified putative WTA synthesis genes for the linkage unit and the polyribitol backbone based on homology to enzymes whose roles in the WTA synthesis pathways of other Gram-positive bacteria have been clearly demonstrated. Unfortunately, bioinformatics analysis did not unambiguously identify the GTs involved in the transfer of α-GlcNAc to the backbone β-GlcNAc.. Nevertheless, our results identified a new *Listeria* WTA glycotype produced by *L. innocua* ŽM39, highlighting the incredible potential diversity of glycostructures in the *Listeria* surfactome.

4. Experimental

4.1. Bacterial strain and growth conditions

The food isolate *Listeria innocua* strain ŽM39 was obtained from the ZIM Culture Collection (University of Ljubljana). This strain is biofilm proficient and suitable for genomic manipulation [32]. For cell wall sacculi isolation, bacteria were cultivated in Miller's lysogeny broth (Miller LB) at 37 °C at 110 rpm. Genomic DNA was isolated from overnight Miller LB agar plate cultures.

4.2. Cell wall sacculi preparation and extraction of cell wall teichoic acids

L. innocua were cultured in Miller LB broth, at 37°C with shaking. Exponentially growing bacterial cultures were harvested by centrifugation (7000 x g, 20 min, 4 °C), and bacteria were resuspended in cold sterile distilled water to OD_{600} = 2.0. After heat inactivation (95 °C, 30 min), bacteria were harvested by centrifugation (14000 x g, 10 min, 25 °C) and resuspended in sterile distilled water. Bacteria were then sonicated twice on ice (cycle 0.9, amplitude 90, time 5 min, UP200S ultrasonic processor; Hielscher) and cell debris was removed by centrifugation 1000 x g, 5 min, 4 °C. Cell wall sacculi were then harvested by centrifugation (20000 x g, 30 min, 4 °C), the pellet was washed once using sterile distilled water and was finally resuspended in SM buffer (100 mM NaCl, 5 mM $MgSO_4$ and 50 mM Tris-HCl pH 7.5). DNase (0.1 mg/mL) and RNase (0.1 mg/mL) treatment was carried out at 37 °C for 4 h followed by proteinase K (0.1 mg/mL) treatment at 37 °C for 16 h with gentle mixing. The cell wall sacculi were harvested by centrifugation (20000 x g, 30 min), resuspended in 4 % SDS and incubated for 30 min at 95 °C. The SDS was removed by centrifugation (20000 x g, 30 min) and the pellet was washed five times using sterile distilled water. The pellet was then sequentially washed with 100 mM EDTA pH 8, water, acetone and water, recovered by lyophilization and stored at -20 °C.

Extraction of WTA was obtained following the protocol of Kho et al., [33]. The sample (30 mg) was initially subjected to acid hydrolysis by addition of 10 mL 10% (w/v) trichloroacetic acid, left under stirring for 18 h at 10 °C and then centrifuged at 5500 x g for 45 min. The pellet was separated from the supernatant and 1 mL of 3 M sodium acetate pH = 5.1 was added to 10 mL of supernatant; then the sample was dried in a rotary evaporator, resuspended in 1.25 mL of water and subsequently added to 5 mL of cold ethanol. After incubation at -20 °C for 16 h, the sample was centrifuged at 5500 x g for 30 min, the supernatant was discarded and the pellet was washed five

294 times with a few mL of ethanol. After the last centrifugation, the pellet was dissolved in 0.5 mL of
295 water and then lyophilized.
296
297 *4.3. Purification and composition analysis of cell wall teichoic acids*
298
299 The WTA extract was subjected to medium pressure size exclusion chromatography on a
300 Bioline chromatography system using a Sephacryl S-300 HR column (1 cm i. d. X 45 cm)
301 connected to a Smartline 1050 pump (Knauer). Elution was carried out with 0.15 M NaCl using a
302 flow rate of 1 mL/min and monitored with a refractive index detector (Smartline 2300, Knauer,
303 Lab-Service Analitica) which was interfaced with a computer via Clarity software. Fractions were
304 collected at 30 s interval; those belonging to the central part of the peak were pooled together and
305 used for the structural determination of WTA. The Sephacryl S-300 HR column was calibrated with
306 pullulan standards of molecular mass (MM) 5900, 11800, 22800, 47300, 112000, 212000, and
307 404000 (Polymer Laboratories, Germany).
308 Composition analysis was determined by GLC of trimethylsilyl methyl glycosides derivatives
309 which were obtained by methanolysis of 0.5 mg of WTA sample with 2 M HCl in methanol at 85
310 °C for 16 h followed by derivatization with the reagent Sylon™ HTP (Sigma) [34].
311 Monosaccharide standards were derivatized in the same way and used to identify the sugars in the
312 WTA sample.
313
314 *4.4. General procedures*
315
316 Analytical GLC was performed on a Perkin-Elmer Autosystem XL gas chromatograph
317 equipped with a flame ionisation detector and using He as the carrier gas. An HP-1 capillary
318 column (Agilent Technologies, 30 m) was used to separate trimethylsilyl methyl glycosides (TMS)
319 with the temperature program: 150–280 °C at 3 °C/min. Identification of the monosaccharides in
320 the WTA sample was achieved by comparison with gas-chromatograms of standards.
321
322 *4.5. NMR spectroscopy*
323
324 Five mg of WTA sample produced by *L. innocua* were exchanged twice with 99.9% D_2O by
325 lyophilization, dissolved in 0.6 mL of 99.96% D_2O and introduced into a 5 mm NMR tube for data
326 acquisition. Spectra were recorded on a 500 MHz VARIAN spectrometer operating at 25 °C, after
327 calibrating the proper pw90° pulse. 1D TOCSY spectra were acquired using mixing times of 80,

100 and 150 ms. 2D experiments were performed using standard VARIAN pulse sequences and pulsed field gradients for coherence selection when appropriate. HSQC spectra were recorded using 145 Hz (for directly attached $^{1}H–^{13}C$ correlations) and a mixing time of 80 ms for the HSQC-TOCSY experiment. $^{1}H–^{13}C$ HMBC experiments were recorded using a coupling constant of 6 Hz (for long range $^{1}H–^{13}C$ correlations) and a relaxation time 1.2 s. TOCSY spectra were acquired using 150 ms mixing time and a 1.2 s relaxation time. $^{1}H-^{31}P$ HMBC experiment was recorded using a coupling constant of 10 Hz. Chemical shifts are expressed in ppm using acetone as internal reference (2.225 ppm for ^{1}H and 31.07 ppm for ^{13}C). NMR spectra were processed using MestreNova software.

4.6. Genomic DNA extraction, sequencing and genome content analysis

Listeria innocua ŽM39 genomic DNA was extracted using QiaAmp DNA Minikit (Qiagen, 51304). Paired end libraries were generated with Nextera XTL library preparation kit (Illumina) according to the manufacturer instructions. Libraries were sequenced using the MiSeq platform. Quality read trimming and adapter removal was achieved using Trimmomatic [35]. Trimmed reads were assembled by Spades [36] and contigs were reordered by Abacas [37]. Plasmid presence was tested in whole genome sequence and sequencing reads using the PlasmidFinder web server [38]. Annotation was carried out by using RASTk on PATRIC server [39, 40]. Predicted proteins were further analysed by Interproscan [41] and additional protein domains were identified by hmm-search [42] against the Pfam database [43]. Prophage sequences were identified using Phaster web server [44].

Putative protein localization was predicted by pSORT web server [45]. Carbohydrate active enzymes were predicted using web dbCan meta server and hmm algorithm (e-value above $1e^{-15}$ and coverage above 0,35) [46]. WTA gene cluster was identified using list of WTA synthesis associated proteins listed in Supplemental Table S1 and stand-alone blastp (e-value above 0,01 and coverage above 30 %) [47]. Protein was considered to be homologous, if the predicted domain responsible for its activity was conserved.

Declaration of competing interest

The authors declare that they have no known competing financial interests or personal relationships that could have appeared to influence the work reported in this paper.

Appendix A. Supplementary data

Acknowledgements

This work was supported by the Scientific and Technological Cooperation Agreement between the Government of the Italian Republic and the Government of the Republic of Slovenia, project # 9: "Mechanism of KKP lectin targeting biofilm of pathogenic and probiotic bacteria", and The Slovenian Research Agency with grants no. J4-9299, P4-0127, and J4-1771.

Appendix A. Supplementary data

Supplementary data to this article can be found online

References

[1] EFSA and ECDC (2019). The European Union one health 2018 zoonoses report. EFSA J. 17:5926. doi: 10.2903/J.Efsa.2019.5926

[2] E.C. Friedly, P.G. Crandall, S. Ricke, C.A. O'Bryan, E.M. Martin, L.M. Boyd, 2008. Identification of *Listeria innocua* surrogates for *Listeria monocytogenes* in hamburger patties. J. Food Sci. 73, M174–M178. https://doi.org/10.1111/j.1750-3841.2008.00719.x.

[3] J. Chen, Q. Chen, L. Jiang, C. Cheng, F. Bai, J. Wang, F. Mo, W. Fang, 2010. Internalin profiling and multilocus sequence typing suggest four *Listeria innocua* subgroups with different evolutionary distances from *Listeria monocytogenes*. BMC Microbiol 10, 97. https://doi.org/10.1186/1471-2180-10-97.

[4] A.B. Silva-Angulo, S.F. Zanini, A. Rosenthal, D. Rodrigo, G. Klein, A. Martínez, 2015. Comparative study of the effects of citral on the growth and injury of *Listeria innocua* and *Listeria monocytogenes*. Cells. PLoS ONE 10(2), e0114026. https://doi.org/10.1371/journal.pone.0114026.

[5] A. Costa, A. Lourenco, T. Civera, L. Brito, *Listeria innocua* and *Listeria monocytogenes* strains from dairy plants behave similarly in biofilm sanitizer testing, LWT 92 (2018) 477–483. https://doi.org/10.1016/j.lwt.2018.02.073.

[6] V. Mohan, R. Wibisono, L. de Hoop, G. Summers, G.C. Fletcher, 2019. Identifying suitable *Listeria innocua* strains as surrogates for *Listeria monocytogenes* for horticultura products. Front. Microbiol. 10, 2281. https://doi.org/10.3389/fmicb.2019.02281.

[7] N. Janež, B. Škrlj, M. Sterniša, A. Klančnik, J. Sabotič (2021) The role of the *Listeria monocytogenes* surfactome in biofilm formation. Microb. Biotechnol. 14(4), (2021) 1269–1281. https://doi.org/10.1111/1751-7915.13847.

[8] A.Ch. Stratakos, U. Zeeshan Ijaz, P. Ward, M. Linton, C. Kelly, L. Pinkerton, P. Scates, J. McBride, I. Pet, A. Criste, D. Stef, J.M. Couto, W.T. Sloan, N. Dorrell, B.W. Wreng, L. Stef, O. Gundogdu, N. Corcionivoschi, 2020. *In vitro* and *in vivo* characterisation of *Listeria monocytogenes* outbreak isolates. Food Control. 107, 106784. https://doi.org/10.1016/j.foodcont.2019.106784

[9] E.T. Sumrall, A.P. Keller, Y. Shen, M.J. Loessner, Structure and function of *Listeria* teichoic acids and their implications, Mol. Microbiol., 113(3) (2020) 627–637. https://doi.org/10.1111/mmi.14472.

[10] C. Weidenmaier, A. Peschel, Teichoic acids and related cell-wall glycopolymers in Gram-positive physiology and host interactions, Nat. Rev. Microbiol. 6 (2008) 276–287. https://doi.org/10.1038/nrmicro1861.

[11] Y. Shen, S. Boulos, E. Sumrall, B. Gerber, A. Julian-Rodero, M.R. Eugster, L. Fieseler, L. Nyström, M.O. Ebert, M.J. Loessner, Structural and functional diversity in *Listeria* cell wall teichoic acids, J. Biol. Chem., 292(43) (2017) 17832–17844. https://doi.org/10.1074/jbc.M117.813964.

[12] F. Fiedler, J. Seger, A. Schrettenbrunner, H.P.R. Seeliger, The biochemistry of murein and cell wall teichoic acids in the genus of *Listeria*, Syst. Appl. Microbiol. **5** (1984) 360–376. https://doi.org/10.1016/S0723-2020(84)80038-7

[13] F. Fiedler, Biochemistry of the cell surface of *Listeria* strains: a locating general view. Infection 16 (1988) S92–S97. https://doi.org/10.1007/BF01639729.

[14] K. Kamisango, H. Fujii, H. Okumura, I. Saiki, Y. Araki, Y. Yamamura, I. Azuma, Structural and immunochemical studies of teichoic acid of *Listeria monocytogenes*, J. Biochem. 93 (1983) 1401–1409. https://doi.org/10.1093/oxfordjournals.jbchem.a134275

[15] M.R. Eugster, M.C. Haug, S.G. Huwiler, M.J. Loessner, The cell wall binding domain of *Listeria* bacteriophage endolysin PlyP35 recognizes terminal GlcNAc residues in cell wall teichoic acid, Mol. Microbiol. 81(6) (2011) 1419–1432. https://doi.org/10.1111/j.1365-2958.2011.07774.x.

[16] K. Uchikawa, I. Sekikawa, I. Azuma, Structural studies on teichoic acids in cell walls of several serotypes of *Listeria monocytogenes*, J. Biochem. 99 (1986) 315–327. https://doi.org/10.1093/oxfordjournals.jbchem.a135486.

[17] P.A. Spears, E.A. Havell, T.S. Hamrick, J.B. Goforth, A.L. Levine, S.T. Abraham, C. Heiss, P. Azadi, P.E. Orndorff, *Listeria monocytogenes* wall teichoic acid decoration in virulence and cell-to-cell spread, Mol Microbiol. 101(5) (2016) 714–730. https://doi.org/10.1111/mmi.13353.

[18] Y. Yin, H. Yao, S. Doijad, S. Kong, Y. Shen, X. Cai, W. Tan, Y. Wang, Y. Feng, Z. Ling, G. Wang, Y. Hu, K. Lian, X. Sun, Y. Liu, C. Wang, K. Jiao, G. Liu, R. Song, X. Chen, Z. Pan, M.J. Loessner, T. Chakraborty, X. Jiao, 2019. A hybrid sub-lineage of *Listeria monocytogenes* comprising hypervirulent isolates. Nat. Commun. 10, 4283. https://doi.org/10.1038/s41467-019-12072-1

[19] M. Lundborg, G. Widmalm, Structural analysis of glycans by NMR chemical shift prediction, Anal. Chem. 83 (2011) 1514–1517. https://doi.org/10.1021/ac1032534

[20] S.J. Angyal, R. Le Fur, D. Gagnaire, Conformations of acyclic sugar derivatives: Part II. Determination of the conformations of alditol acetates in solution by the use of 250-MHz nmr spectra, Carbohydr. Res. 23 (1972) 121–134. https://doi.org/10.1016/S0008-6215(00)81583-9

[21] S.J. Angyal, R. Le Fur, The ^{13}C-NMR spectra of alditols, Carbohydr. Res. 84 (1980) 201–209. https://doi.org/10.1016/S0008-6215(00)85551-2

[22] P. Glaser, L. Frangeul, C. Buchrieser, C. Rusniok, A. Amend, F. Baquero, P. Berche, H. Bloecker, P. Brandt, T. Chakraborty, A. Charbit, F. Chetouani, E. Couvé, A. De Daruvar, P. Dehoux, E. Domann, G. Domínguez-Bernal, E. Duchaud, L. Durant, O. Dussurget, K.D. Entian, H. Fsihi, F. Garcia-Del Portillo, P. Garrido, L. Gautier, W. Goebel, N. Gómez-López, T. Hain, J. Hauf, D. Jackson, L.M. Jones, U. Kaerst, J. Kreft, M. Kuhn, F. Kunst, G. Kurapkat, E. Madueño, A. Maitournam, J. Mata Vicente, E. Ng, H. Nedjari, G. Nordsiek, S. Novella, B. De Pablos, J.C. Pérez-Diaz, R. Purcell, B. Remmel, M. Rose, T. Schlueter, N. Simoes, A. Tierrez, J.A. Vázquez-Boland, H. Voss, J. Wehland, P. Cossart, Comparative genomics of *Listeria* species, Science 294 (2001) 849–852. https://doi.org/10.1126/science.1063447.

[23] S. Brown, J.P. Santa Maria, S. Walker, Wall teichoic acids of Gram-positive bacteria, Annu. Rev. Microbiol. 67 (2013) 313–336. https://doi.org/10.1146/annurev-micro-092412-155620.

[24] X.H. Lei, F. Fiedler, Z. Lan, S. Kathariou, A novel serotype-specific gene cassette (gltA-gltB) is required for expression of teichoic acid-associated surface antigens in *Listeria monocytogenes* of serotype 4b, J. Bacteriol. 183 (2001) 1133–1139. https://doi.org/10.1128/JB.183.4.1133-1139.2001.

[25] F. Carvalho, M.L. Atilano, R. Pombinho, G. Covas, R.L. Gallo, S.R. Filipe, S. Sousa, D. Cabanes, 2015. L-Rhamnosylation of *Listeria monocytogenes* wall teichoic acids promotes resistance to antimicrobial peptides by delaying interaction with the membrane. PLOS Pathog. 11, e1004919. https://doi.org/10.1371/journal.ppat.1004919.

[26] R. van Dalen, A. Peschel, N.M. van Sorge, Wall teichoic acid in *Staphylococcus aureus* host interaction. Trends in Microbiol. 28 (2020) 985–998. https://doi.org/10.1016/j.tim.2020.05.017.

[27] J. Rismondo, T.F.M. Haddad, Y. Shen, M.J. Loessner, A. Gründling, 2020. GtcA is required for LTA glycosylation in *Listeria monocytogenes* serovar 1/2a and *Bacillus subtilis*. Cell Surf. 6, 100038. https://doi.org/10.1016/j.tcsw.2020.100038.

[28] M.R. Eugster, M.J. Loessner, Wall teichoic acids restrict access of bacteriophage endolysin Ply118, Ply511, and Plyp40 cell wall binding domains to the *Listeria monocytogenes* peptidoglycan, J. Bacteriol. 194 (2012) 6498–6506. https://doi.org/10.1128/JB.00808-12.

[29] Y. Kaya, Y. Araki, E. Ito, Characterization of a novel linkage unit between ribitol teichoic acid and peptidoglycan in *Listeria monocytogenes* cell walls, Eur. J. Biochem. 146 (1985) 517–522. https://doi.org/10.1111/j.1432-1033.1985.tb08682.x.

[30] E.T. Sumrall, S.R. Scheider, S. Boulos, M Loessner, Y. Shen, 2021. Glucose decoration on wall teichoic acid is required for phage adsorption and InlB-mediated virulence in *Listeria ivanovii*. J. Bacteriol. 203, e00136-21. https://doi.org/10.1128/JB.00136-21.

[31] X.H. Lei, F. Fiedler, Z. Lan, S. Kathariou, A novel serotype-specific gene cassette (gltA-gltB) is required for expression of teichoic acid-associated surface antigens in *Listeria monocytogenes* of serotype 4b, J. Bacteriol. 183 (2001) 1133–1139. https://doi.org/10.1128/JB.183.4.1133-1139.2001.

[32] A. Berlec, N. Janež, M. Sterniša, A. Klančnik, J. Sabotič, 2021. Expression of NanoLuc luciferase in *Listeria innocua* for development of biofilm assay. Front. Microbiol. 12, 636421. https://doi.org/10.3389/fmicb.2021.636421.

[33] K. Kho, T.C. Meredith, 2018. Extraction and analysis of bacterial teichoic acids. Bio-protocol, 8, e3078. https://doi.org/10.21769/BioProtoc.3078.

[34] K. Kakehi, S. Honda, Silyl ethers of carbohydrates, in: C.J. Biermann, G.D. McGinnis (Eds.), Analysis of Carbohydrates by GLC and MS, CRC Press, Boca Raton (FL) 1989, pp. 43–85

[35] A.M. Bolger, M. Lohse, B. Usadel, Trimmomatic: A flexible trimmer for Illumina sequence data, Bioinformatics. 30 (2014) 2114–2120. https://doi.org/10.1093/bioinformatics/btu170.

[36] A. Bankevich, S. Nurk, D. Antipov, A.A. Gurevich, M. Dvorkin, A.S. Kulikov, V.M. Lesin, S.I. Nikolenko, S. Pham, A.D. Prjibelski, A. V. Pyshkin, A. V. Sirotkin, N. Vyahhi, G. Tesler, M.A. Alekseyev, P.A. Pevzner, SPAdes: A new genome assembly algorithm and its applications to single-cell sequencing, J. Comput. Biol. 19 (2012) 455–477. https://doi.org/10.1089/cmb.2012.0021.

[37] S. Assefa, T.M. Keane, T.D. Otto, C. Newbold, M. Berriman, ABACAS: Algorithm-based automatic contiguation of assembled sequences, Bioinformatics. 25 (2009) 1968–1969. https://doi.org/10.1093/bioinformatics/btp347.

[38] A. Carattoli, E. Zankari, A. Garciá-Fernández, M.V. Larsen, O. Lund, L. Villa, F.M. Aarestrup, H. Hasman, In Silico detection and typing of plasmids using plasmidfinder and plasmid multilocus sequence typing, Antimicrob. Agents Chemother. 58 (2014) 3895–3903. https://doi.org/10.1128/AAC.02412-14.

[39] T. Brettin, J.J. Davis, T. Disz, R.A. Edwards, S. Gerdes, G.J. Olsen, R. Olson, R. Overbeek, B. Parrello, G.D. Pusch, M. Shukla, J.A. Thomason, R. Stevens, V. Vonstein, A.R. Wattam, F. Xia, 2015. RASTtk: A modular and extensible implementation of the RAST algorithm for building custom annotation pipelines and annotating batches of genomes. Sci. Rep. 5, 8365. https://doi.org/10.1038/srep08365.

[40] A.R. Wattam, J.J. Davis, R. Assaf, S. Boisvert, T. Brettin, C. Bun, N. Conrad, E.M. Dietrich, T. Disz, J.L. Gabbard, S. Gerdes, C.S. Henry, R.W. Kenyon, D. Machi, C. Mao, E.K. Nordberg, G.J. Olsen, D.E. Murphy-Olson, R. Olson, R. Overbeek, B. Parrello, G.D. Pusch, M. Shukla, V. Vonstein, A. Warren, F. Xia, H. Yoo, R.L. Stevens, Improvements to PATRIC, the all-bacterial bioinformatics database and analysis resource center, Nucleic Acids Res. 45 (2017) D535–D542. https://doi.org/10.1093/nar/gkw1017.

[41] P. Jones, D. Binns, H.Y. Chang, M. Fraser, W. Li, C. McAnulla, H. McWilliam, J. Maslen, A. Mitchell, G. Nuka, S. Pesseat, A.F. Quinn, A. Sangrador-Vegas, M. Scheremetjew, S.Y. Yong, R. Lopez, S. Hunter, InterProScan 5: Genome-scale protein function classification, Bioinformatics. 30 (2014) 1236–1240. https://doi.org/10.1093/bioinformatics/btu031.

[42] A. Krogh, M. Brown, I.S. Mian, K. Sjölander, D. Haussler, Hidden Markov Models in computational biology applications to protein modeling, J. Mol. Biol. 235 (1994) 1501–1531. https://doi.org/10.1006/jmbi.1994.1104.

[43] E.L. Sonnhammer, S.R. Eddy, R. Durbin, Pfam: A Comprehensive Database of Protein Domain Families Based on Seed Alignments, Proteins. 28(3) (1997) 405–420. https://doi.org/10.1002/(sici)1097-0134(199707)28:3<405::aid-prot10>3.0.co;2-l.

[44] D. Arndt, J.R. Grant, A. Marcu, T. Sajed, A. Pon, Y. Liang, D.S. Wishart, PHASTER: a better, faster version of the PHAST phage search tool, Nucleic Acids Res. 44 (2016) W16–W21. https://doi.org/10.1093/nar/gkw387.

[45] N.Y. Yu, J.R. Wagner, M.R. Laird, G. Melli, S. Rey, R. Lo, P. Dao, S. Cenk Sahinalp, M. Ester, L.J. Foster, F.S.L. Brinkman, PSORTb 3.0: Improved protein subcellular localization prediction with refined localization subcategories and predictive capabilities for all

prokaryotes, Bioinformatics. 26 (2010) 1608–1615. https://doi.org/10.1093/bioinformatics/btq249.

[46] H. Zhang, T. Yohe, L. Huang, S. Entwistle, P. Wu, Z. Yang, P.K. Busk, Y. Xu, Y. Yin, DbCAN2: A meta server for automated carbohydrate-active enzyme annotation, Nucleic Acids Res. 46 (2018) W95–W101. https://doi.org/10.1093/nar/gky418.

[47] C. Camacho, G. Coulouris, V. Avagyan, N. Ma, J. Papadopoulos, K. Bealer, T.L. Madden, 2009. BLAST+: Architecture and applications. BMC Bioinformatics. 10, 421. https://doi.org/10.1186/1471-2105-10-421.

FIGURE LEGENDS

Fig. 1: ^{1}H NMR spectrum of *L. innocua* ŽM39 WTA recorded at 500 MHz, 25 °C.

Fig. 2: 1D TOCSY spectra of *L. innocua* ŽM39 WTA recorded at 500 MHz, 25 °C obtained with selective excitation of resonances (A) at 3.54 (**A4**), (B) 4.65 (**B1**) and (C) 4.10 (**R1**) ppm and using 100 ms mixing time. (D) For comparison ^{1}H NMR spectrum of *L. innocua* ŽM39 WTA recorded at 500 MHz, 25 °C. Peaks have been labelled as in Table 2.

Fig. 3: ^{1}H–^{13}C HSQC plot of *L. innocua* ŽM39 WTA recorded at 500 MHz, 25 °C. The methyl region is reported in the inset. Proton/carbon cross peaks have been labelled according to the corresponding residue (**A**, **B** and **R**), as in Table 2.

Fig. 4: ^{1}H–^{31}P HMBC plot of *L. innocua* ŽM39 WTA recorded at 500 MHz, 25 °C. Proton/phosphorous cross peaks have been labelled according to the corresponding residue (**A**, **B** and **R**), as in Table 2. Cross peaks marked with a star at 3.97 and 3.91 ppm (^{1}H) are assigned to H1 of Rbo phosphomonoester.

Fig. 5: Schematic representation of the *L. innocua* ŽM39 WTA of type II structure. The repeating unit is composed of the backbone [→4)-β-Glc*p*NAc-(1→4)-Rbo-(1→P) with an α-Glc*p*NAc residue bound to C3 of β-Glc*p*NAc, as determined in the present study. The linkage unit is illustrated based on the structure determined by Kaya et al. (1985) [29].

Table 1
Serovars, repeating unit structures and substituents of *Listeria* type I and type II WTAs, including *L. innocua* WTA

Serovars	Major repeating unit structures	Substituents [a]	Ref
	Type I		
1/2	[→5)-[α-D-Glc*p*NAc-(1→2)][α-L-Rha*p*-(1→4)]-D-Rbo-(1P→]$_n$		[9, 14]
1/2*	[→5)-[α-L-Rha*p*-(1→4)]-D-Rbo-(1P→]$_n$		[9, 15]
3	[→5)-[α-D-Glc*p*NAc-(1→2)]-D-Rbo-(1P→]$_n$		[16]
7	[→5)-[α-D-Hex*p*-(1→2 or 4)]-D-Rbo-(1P→]$_n$		[11]
	Type II		
4a	[→4)-β-D-Glc*p*NAc-(1→2)-D-Rbo-1P→]$_n$	partial GlcNAc3Ac	[16]
4b	[→4)-[α-D-Gal*p*-(1→6)][β-D-Glc*p*(1→3)]-β-D-Glc*p*NAc-(1→4)-D-Rbo-1P→]$_n$	Non-stoichiometric Gal and Glc; some Glc replaced by GlcNAc3Ac	[11, 16]
4c	[→4)-[α-D-Gal*p*-(1→6)]-β-D-Glc*p*NAc-(1→2)-D-Rbo-1P→]$_n$	partial GlcNAc3Ac	[11, 17]
4d	[→4)-[β-D-Glc*p*-(1→3)]-β-D-Glc*p*NAc-(1→4)-D-Rbo-1P→]$_n$	Non-stoichiometric Glc; some Glc replaced by GlcNAc3Ac	[11, 16]
4d*	[→4)-β-D-Glc*p*NAc-(1→4)-D-Rbo-1P→]$_n$	partial GlcNAc3Ac	[9]
4e	[→4)-[α-D-Gal*p*-(1→6)][D-Glc*p*-(1→3)]-β-D-Glc*p*NAc-(1→4)-D-Rbo-1P→]$_n$	Non-stoichiometric Gal and Glc; Glc replaced by GlcNAc3Ac	[18]
4h	[→4)-[α-D-Gal*p*-(1→6)]-β-D-Glc*p*NAc-(1→4)-D-Rbo-1P→]$_n$	Non-stoichiometric Gal; partial GlcNAc3Ac	[11]
5/6b	[→4)-[D-Glc*p*-(1→3)]-β-D-Glc*p*NAc-(1→2)-D-Rbo-1P→]$_n$	Non-stoichiometric Glc, some Glc replaced by GlcNAc3Ac	[11]
6a [b]	[→4)-[D-Gal*p*-(1→6)][D-Glc*p*NAc-(1→3)]-D-Glc*p*NAc-(1→4)-D-Rbo-1P→]$_n$	Non-stoichiometric Gal and GlcNAc, partial GlcNAc3Ac	[11]
NA	[→4)-[α-D-Glc*p*NAc-(1→3)]-β-D-Glc*p*NAc-(1→4)-D-Rbo-(1P→]$_n$		This work

[a] Degree of acetylation is reported always below 100%. [b] Anomeric configuration of sugar residues for WTA serovar 6a is not reported in the literature.
NA = not applicable

Table 2
^{1}H and ^{13}C chemical shift assignments of *Listeria innocua* ŽM39 WTA recorded at 500 MHz and 25 °C.

Residue	Nucleus	Chemical shifts (ppm) [a]					
		1	2	3	4	5	6
A	^{1}H	5.14	3.87	3.80	3.54	3.72	3.83 - 3.79
α-D-Glc*p*NAc-(1→	^{13}C	99.2 (+7.4)	54.9	71.2	70.1	73.6	60.6
B	^{1}H	4.65	3.88	3.84	4.24	3.62	3.85 - 3.96
→3,4)-β-D-Glc*p*NAc-(1→	^{13}C	101.9 (+5.0)	56.0	<u>80.9</u> (+6.1)	<u>74.7</u> (+3.6)	75.6	61.3
R	^{1}H	4.10 - 3.99	3.82	3.82	3.91	3.78 – 3.86	
→4)-Rbo-(1P→	^{13}C	67.3 (+3.5)	70.9	71.7	<u>82.7</u> (+9.1)	61.5	

[a] Chemical shifts are given relative to internal acetone (2.225 ppm for ^{1}H and 31.07 ppm for ^{13}C). Linkage carbon atoms are identified by glycosylation shifts in brackets and those detected in the HMBC plots are underlined.

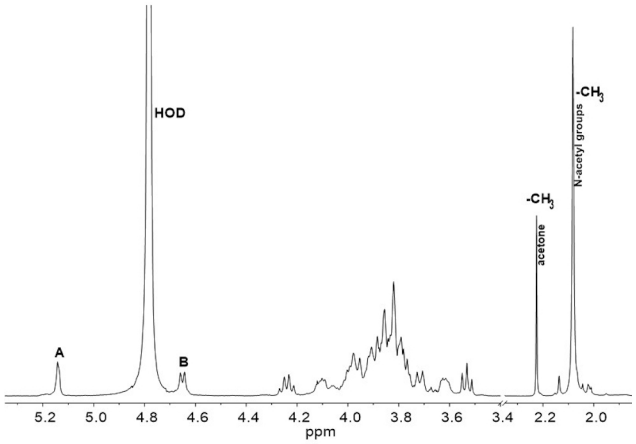

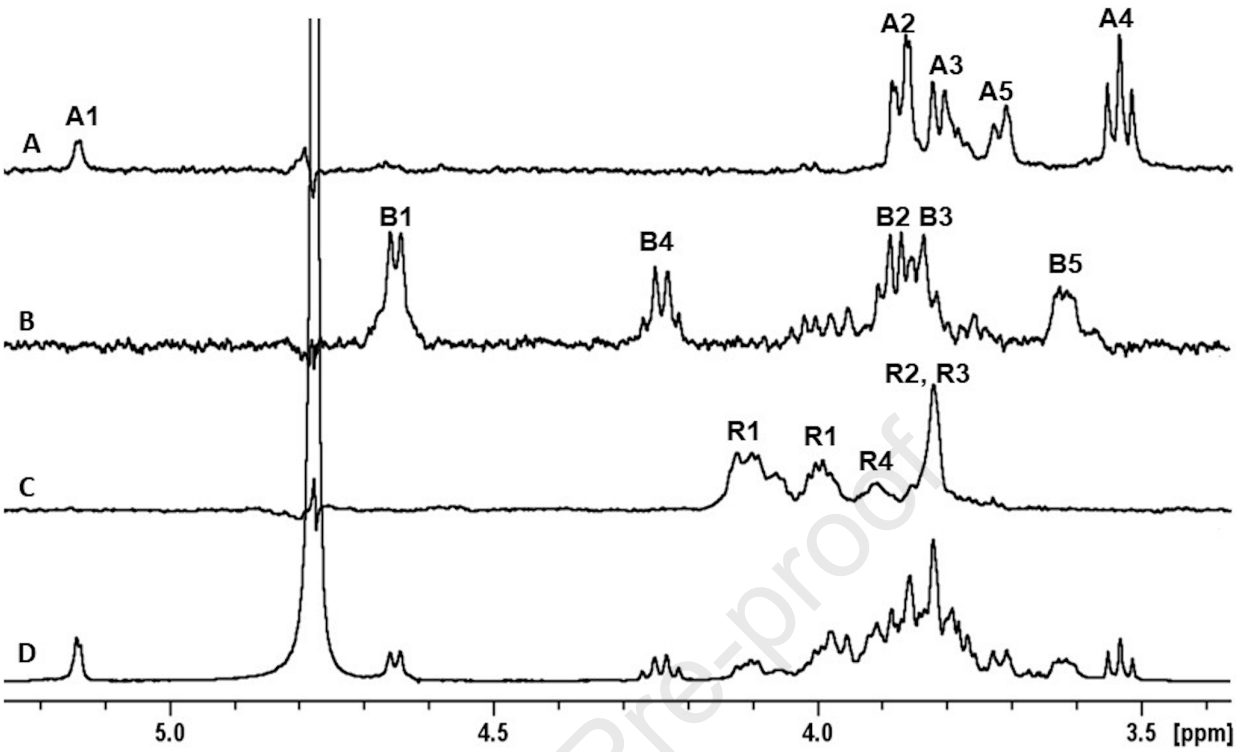

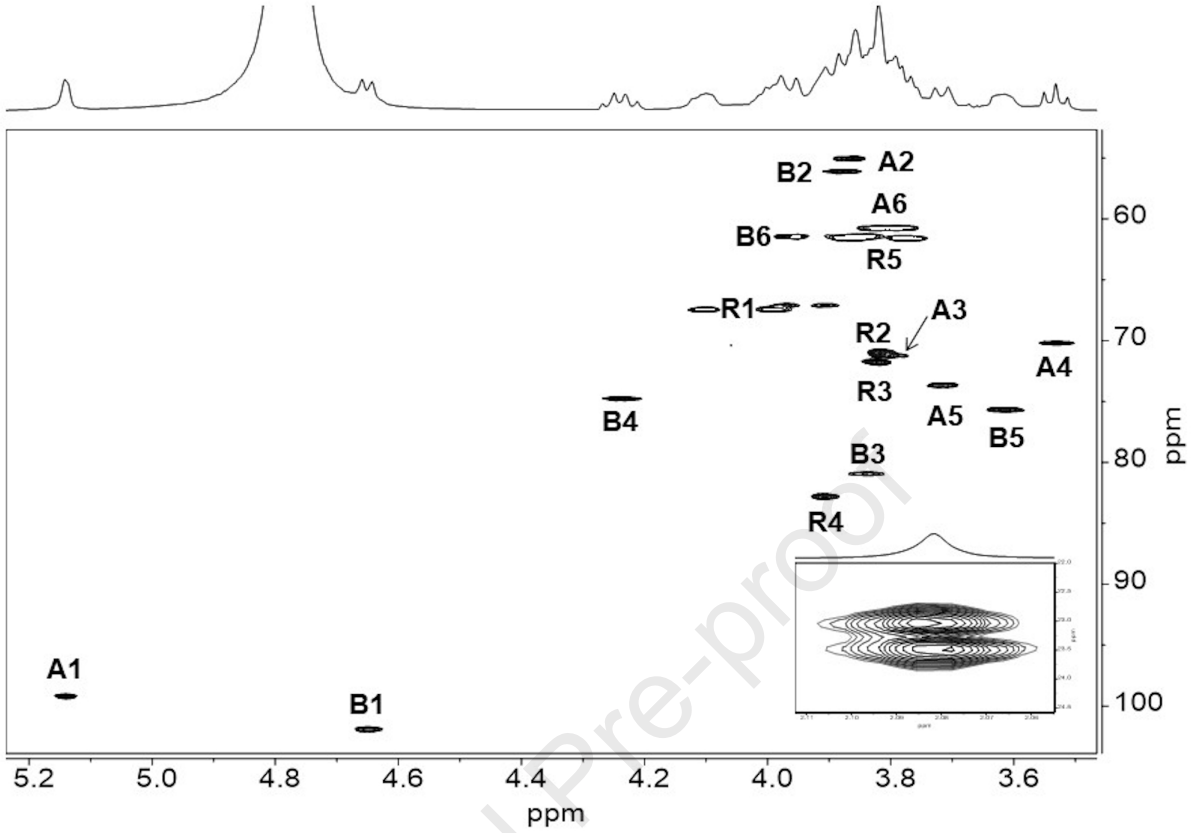

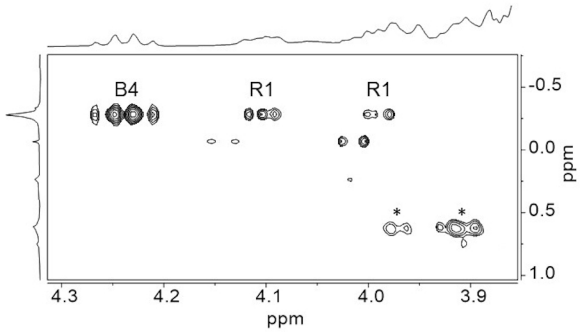

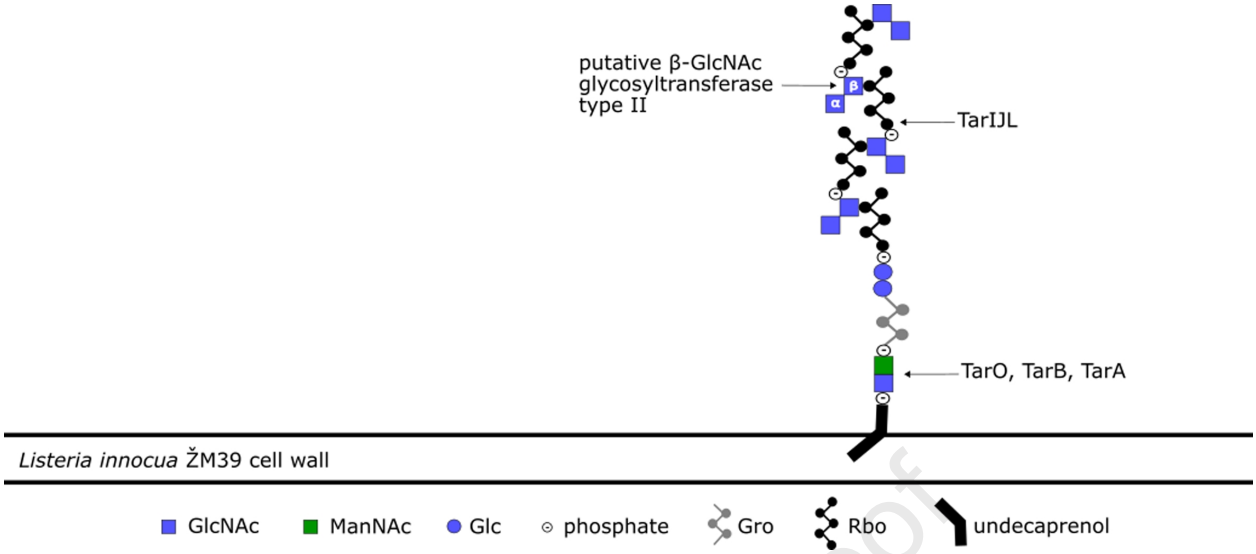

Highlights

- WTA was isolated from the foodborne *Listeria innocua* ŽM39 strain
- The structure of the *L. innocua* ŽM39 WTA was determined by NMR to be new
- In *L. innocua* WTA the disaccharide α-GlcNAc-(1→3)-β-GlcNAc is linked to C4 of Rbo
- Putative WTA synthesis genes were identified in the genome

Declaration of interests

☒ The authors declare that they have no known competing financial interests or personal relationships that could have appeared to influence the work reported in this paper.

☐The authors declare the following financial interests/personal relationships which may be considered as potential competing interests: